

Geometrical structures and molecular adsorption reactions of alkali-halide cluster ions investigated by ion mobility-mass spectrometry

Salt Production

Abstract

Structures of small sodium halide nanocrystal (cluster) cations and anions, $\text{Na}_n\text{F}_{n-1}^+$, $\text{Na}_n\text{I}_{n-1}^+$, $\text{Na}_{n-1}\text{F}_n^-$, and $\text{Na}_{n-1}\text{I}_n^-$, have been studied by ion mobility mass spectrometry coupled with quantum chemical calculations. In this spectrometry, structural information of atomic and molecular cluster ions was obtained from the measurement of collision cross sections of the ions with a buffer gas in an ion drift cell. As a result of the comparison between the experimental cross sections thus measured and those obtained by theoretical calculations, it was found that the $\text{Na}_n\text{F}_{n-1}^+$ cluster ions have substructures of bulk face-centered-cubic crystals in most of the cluster size. Among such structures, we predominantly observed cuboid ions with near regular hexahedron such as $n = 14$ ($3 \times 3 \times 3$) and 23 ($3 \times 3 \times 5$) as magic numbers in the mass spectra. In addition, non-rock-salt “cage” type structures in which one sodium atom is encapsulated into the sodium fluoride cuboid lattice were also found to be stable for $n = 7$ and 10 . Also the stable geometric structures of above four cluster systems were examined systematically in order to obtain the dependence of composite ion sizes on the stable structures. As for the $\text{Na}_{n-1}\text{F}_n^-$ anions and the $\text{Na}_n\text{I}_{n-1}^+$ cations, cage type structures similar to those of Na_7F_6^+ and $\text{Na}_{10}\text{F}_9^+$ were observed at $n = 7$ and 10 . However, similar cage structures were not detected for $n = 7$ and 10 of $\text{Na}_{n-1}\text{I}_n^-$ anions. This result indicates that the cage structures are sensitive to the radius of caged ions (excess atomic ions): Inclusion of I^- (ionic radius of 2.06 \AA) causes large distortion in the structure, whereas they are stable for small caged ions such as Na^+ (1.16 \AA) and F^- (1.19 \AA). The experiment of water and methanol adsorption reactions on $\text{Na}_n\text{F}_{n-1}^+$ ions also showed that the water molecule is highly reactive at specific cluster size, e.g., $n = 13$ and 22 .

Keywords: Nanocrystal, Cluster, Adsorption reaction, Sodium halide, Mass spectrometry, Ion mobility spectrometry

Introduction

Clusters, defined as small aggregates of up to several hundreds of atoms or molecules, are considered as microscopic model systems of bulk phases. Because of this importance, the clusters have been studied extensively especially as a function of the number of constituent particles, that is, the cluster size. In particular, size-selected alkali halide clusters in the gas phase have been investigated by spectroscopic and mass spectrometric techniques for more than 30 years in addition to theoretical calculation studies [1-28]. As a result, the following knowledge was already obtained: (1) The cluster consists of alkali cations and halogen anions. In a sodium fluoride cluster, for example, a neutral cluster has a predominant composition of Na_nF_n , whereas the positive and negative ions have forms of $\text{Na}_n\text{F}_{n-1}^+$ and $\text{Na}_{n-1}\text{F}_n^-$, respectively. (2) The cluster has a stable geometry which is close to a partial structure of bulk rock-salt-type, face-centered-cubic crystals. That is, the cluster becomes a good model of the bulk crystal. For this reason, this cluster is often called a nanocrystal. (3) Among the structures similar to bulk crystals, perfect cuboid structures are extraordinarily stable because of the minimum surface energy. A variety of cluster size n can constitute the cuboid structures for neutral clusters such as Na_nF_n . However, cuboids only form for ionic clusters, e.g. $\text{Na}_n\text{F}_{n-1}^+$ and $\text{Na}_{n-1}\text{F}_n^-$ for a limited number of values of n . For example in $\text{Na}_n\text{F}_{n-1}^+$, the $(j \times k \times l)$ cuboid

structure (j, k, l indicates the number of atoms of each side) is formed only if all of the numbers $j, k,$ and l are odd, because the number of Na^+ ions are one more than that of F^- . Thus the cuboid structures are only formed for the sizes such as $n = 14$ ($3 \times 3 \times 3$), 23 ($3 \times 3 \times 5$), and 38 ($3 \times 5 \times 5$). The ions with these n values were actually observed to have higher intensities than those with adjacent cluster sizes in mass spectrum (magic numbers). (4) From the studies of adsorption reactions [6,9,18,28], high reactivity was observed for the sizes n with one smaller than those forming cuboid structures. This observation was explained by the fact that the defect structures serve highly reactive adsorption sites, and the fact was also supported by the results of theoretical calculations.

In the present study, stable structures were first assigned for cluster cations and anions of sodium fluoride and sodium iodide by ion mobility mass spectrometry (IM-MS). As noted above, water adsorption on alkali halide clusters gives a model of initial stage of dissolution or deliquescence of bulk salt crystals. Therefore, in addition to the structure analysis of bare cluster ions, we also discussed the adsorption reactivity on the sodium fluoride cations by observing collisional reactions with water or methanol using the same experimental setup. The IM-MS, which is a combination of ion mobility spectrometry (IMS) and mass spectrometry (MS), is a powerful technique for determining the structures of gas-phase ions [29-32]. In a conventional drift-tube type IMS, pulsed ions are injected into an ion-drift cell in which buffer gas such as He is introduced and the electric field is applied so as to accelerate ions downstream. In the ion-drift cell, due to a balance of acceleration of ions by the electric field, E , and deceleration by collisions with buffer gas atoms, a drift velocity of the ions, v_d , becomes a constant value proportional to E , i.e.,

$$v_d = KE, \quad (1)$$

in which the coefficient K is termed the ion mobility. The mobility K of thermalized ions drifting through the buffer gas under the weak electric field was given from the kinetic theory of ion transport [29,30] as:

$$K = \frac{3e}{16N} \left(\frac{2\pi}{k_B \mu T_{\text{eff}}} \right)^{1/2} \frac{1}{\Omega^{(1,1)}}, \quad (2)$$

where e is the elementary charge, N is the number density of the buffer gas atoms, k_B is the Boltzmann constant, μ is the reduced mass of the ion and the buffer gas atom, and $\Omega^{(1,1)}$ is a collision integral representing an average over collision energy, orientations and inelastic collisions. When we treat the ion and neutral as hard spheres without internal states, $\Omega^{(1,1)}$ reduces to the hard-sphere collision cross section, Ω . Although the eq. (2) was derived for the collisions of atomic ions with atoms, this equation has been widely applied to the system of polyatomic ions in the buffer gas atoms. The term T_{eff} , the effective temperature of the ions, is given by $T_{\text{BG}} + m_B v_d^2 / 3k_B$, where T_{BG} is the buffer gas temperature and m_B is the mass of buffer gas. From eqs. (1) and (2), the time that the ion spends in the ion-drift cell is thus inversely proportional to K and directly proportional to Ω . Therefore, Ω was evaluated by measuring the v_d of the ions in the ion-drift cell. The collision cross section (collision integral) can also be determined for the ion structures optimized in a quantum chemical calculations. From the comparison of the experimental and theoretical cross sections, we assigned the structure of each cluster ion observed in the present measurement.

Experimental and calculation details

Experiment was performed with a five-stage differentially evacuated vacuum chambers containing a cluster ion source, an ion drift cell for mobility spectrometry, and a reflectron-type time-of-flight mass spectrometer (TOF-MS), as shown in Fig. 1. The setup was already reported in detail elsewhere [33-35]. Sodium fluoride/iodide cluster cations and anions were

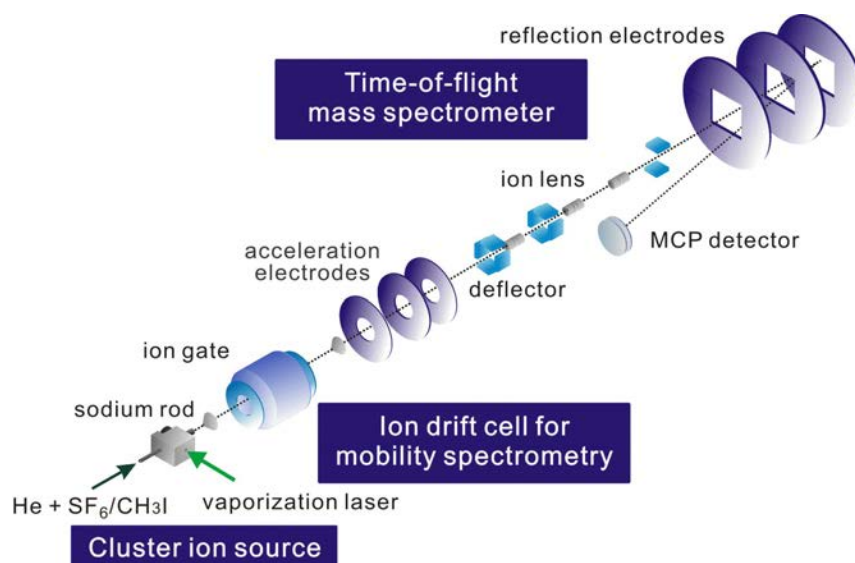


Fig. 1. Schematic view of the present experimental apparatus.

produced by laser vaporization of a sodium rod and subsequent reaction with SF_6/He or $\text{CH}_3\text{I}/\text{He}$ mixed gas from a pulsed valve. The generated cluster ions were injected into the ion-drift cell with a kinetic energy of 50 eV by a pulsed electric field. The ion-drift cell was filled with He buffer gas at 0.80 Torr and was cooled to 180 K. After exiting the cell, the ions were re-accelerated in an acceleration region of the reflectron TOF-MS at a given time Δt later from the ion-injection pulse. This delay time, Δt , was hereafter denoted as “arrival time”. Finally the ions were mass-analyzed by the TOF mass spectrometer. In the IM-MS measurement, we obtained a series of TOF mass spectra sequentially by scanning Δt . As a result, cluster ions with different cross sections were separately detected at different arrival times in a two-dimensional plot of TOF vs. arrival time.

The collision cross section Ω between the ion and a He atom was determined from this measurement using eqs. (1) and (2). The ion flight time in the drift cell t_d was first determined by subtracting the time flying the outside regions of the cell, which was calculated with solving the equations of motion of the ions, from the peak of the arrival time distribution of the ion. Then the drift velocity v_d and thus the ion mobility K were determined from t_d and eq. (1). Finally Ω was determined from the eq. (2). A TOF mass spectrum was also obtained from the two-dimensional plot of TOF vs. arrival time noted above. In the present apparatus, after injection into the cell by a pulsed electric field, cluster ions diffuse spatially in their running direction depending on their cross sections before reaching the acceleration region of the TOF mass spectrometer. Therefore, the TOF mass spectrum was obtained by summing up all the TOF spectra measured at every arrival time because of the spread of arrival time distribution of the cluster ions.

In the molecular adsorption experiment, the ion-drift cell was filled with He buffer gas and a small amount of the reaction gas (water: 0.2% and methanol: 1%). The total pressure and the temperature of the drift cell were fixed at 0.80 Torr and at room temperature.

Quantum chemical calculations for the geometry optimizations of sodium fluoride and sodium iodide cluster ions were performed prior to calculations of collision integrals which can be compared with the collision cross sections of the ions. The geometry optimizations were carried out with M06-2X/aug-cc-pVDZ-pp level in Gaussian 09 [36]. The singlet spin state was considered in these calculations. The collision integral of the ion with a He atom was calculated by the trajectory method which is included in the MOBCAL program [37].

Results and discussion

Geometrical structures of sodium halide cluster cations and anions

As noted in the experimental section, collision cross sections of sodium halide cluster ions with helium buffer gas were determined by ion mobility mass spectrometry. Fig. 2 shows the plots of cross sections for sodium fluoride and sodium iodide cluster cations and anions, $\text{Na}_n\text{F}_{n-1}^+$, $\text{Na}_n\text{I}_{n-1}^+$, $\text{Na}_{n-1}\text{F}_n^-$, and $\text{Na}_{n-1}\text{I}_n^-$, with n up to 23 for sodium fluoride and 14 for sodium iodide. Following features were observed from this figure: (1) The collision cross section increased with increasing cluster size in all sodium halide ion systems, whereas the increment was dependent upon the system. (2) The sodium fluoride clusters $\text{Na}_n\text{F}_{n-1}^+$ and $\text{Na}_{n-1}\text{F}_n^-$ had a common tendency that the cross sections reached ceilings at $n = 4, 7, 10, 14$, and 19. (3) The peaking trend observed in NaF systems noted in (2) was not discernable in NaI cluster ions. However, the cross sections hit the maxima at $n = 7$ and 10 for $\text{Na}_n\text{I}_{n-1}^+$ ions. (4) In $\text{Na}_{n-1}\text{I}_n^-$, no tendency reaching ceilings at $n = 7$ and 10 which were observed in the other systems were not observed in Fig. 2.

In order to discuss the above observed features from geometrical structures of the nanocrystal ions, the collision integrals with a He atom were calculated independently for the most stable structures optimized by quantum chemical calculations as note in the Experimental and calculation details section. The results were also plotted in Fig. 2 as Ω_{calc} . As a result, the Ω_{calc} values were found to agree with Ω_{exp} within errors except for $\text{Na}_n\text{I}_{n-1}^+$ ion systems. On the other hand, discrepancies were obtained between experimental and theoretical cross sections in $\text{Na}_n\text{I}_{n-1}^+$. The source of the gap observed for Ω_{exp} and Ω_{calc} in $\text{Na}_n\text{I}_{n-1}^+$ was not clear at present, however, we concluded that all of the ions examined in the present study was explained by the most stable structures, because the detailed size dependence was consistent between Ω_{exp} and Ω_{calc} even in the $\text{Na}_n\text{I}_{n-1}^+$ ions.

Most of the assigned stable structures have the same geometry for the above four sodium halide cluster cations and anions. Such structures have partial structures of rock-salt type crystals. However, we reported that the $\text{Na}_n\text{F}_{n-1}^+$ ions with $n = 7$ and 10 have characteristic “cage”-type, non-rock-salt structures in which one sodium atom is encapsulated into the sodium fluoride cuboid lattice [34]. In the present study the structures at these sizes were compared for the four different

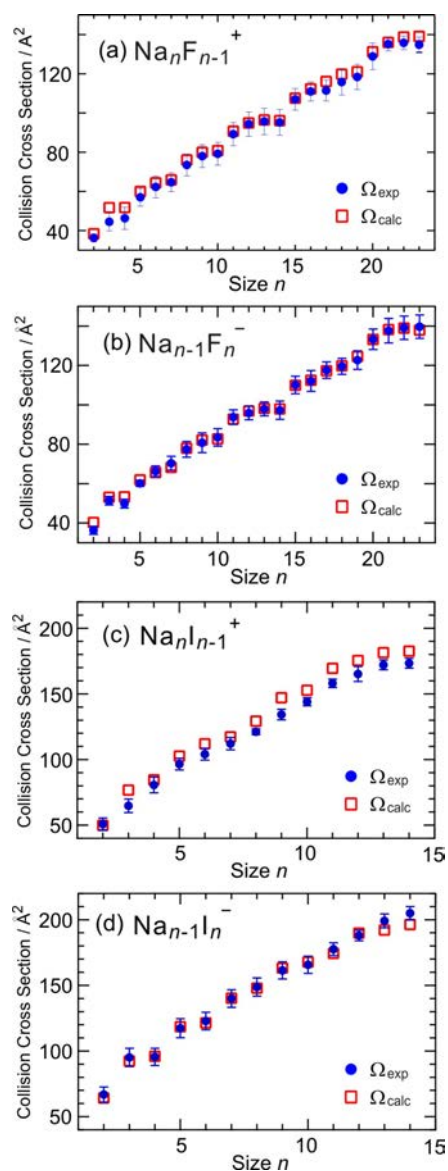


Fig. 2. Collision cross sections of (a) $\text{Na}_n\text{F}_{n-1}^+$, (b) $\text{Na}_{n-1}\text{F}_n^-$, (c) $\text{Na}_n\text{I}_{n-1}^+$, and (d) $\text{Na}_{n-1}\text{I}_n^-$. (a) and (b); $n = 2-23$, (c) and (d); $n = 2-14$.

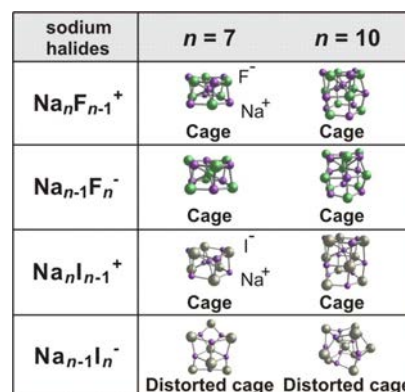


Fig. 3. Assigned structures of sodium halide cluster ions for $n = 7$ and 10.

sodium halide cluster cations and anions, as summarized in Fig. 3. The result indicated that the “cage” structures similar to $\text{Na}_n\text{F}_{n-1}^+$ were obtained for $n = 7$ and 10 of $\text{Na}_{n-1}\text{I}_{n-1}^+$ and $\text{Na}_{n-1}\text{F}_n^-$. As noted above, these structures are compact with relatively small collision cross sections. Although the ions of $\text{Na}_{n-1}\text{I}_n^-$ also have cage structures at $n = 7$ and 10 , those were found to have fairly distorted structures than other systems. In fact these structures were no longer compact, and thus there were no tendency reaching ceilings at $n = 7$ and 10 . This difference can be explained by the large ionic radius of the I⁻ ion which should be encapsulated in $\text{Na}_{n-1}\text{I}_n^-$ compared with the radii of other atomic ions, Na⁺ and F⁻: The radius of I⁻, 2.06 Å, was nearly twice of the radius of Na⁺ (1.16 Å) or F⁻ (1.19 Å) [38], and therefore, the $\text{Na}_{n-1}\text{I}_n^-$ cluster ions had distorted structures at $n = 7$ and 10 in order to keep the cage structures.

Size dependence of adsorption reactivity of water and methanol molecules

Fig. 4 shows TOF mass spectra of $\text{Na}_n\text{F}_{n-1}^+$ reacted with H₂O and CH₃OH in addition to bare cluster ions, all of which were obtained from the 2D plots of TOF and arrival time. Magic numbers were observed for bare $\text{Na}_n\text{F}_{n-1}^+$ cluster ions in these mass spectra, such as $n = 14$ (3×3×3) and 23 (3×3×5). Water- or methanol-adsorbed ions were also observed for limited cluster sizes which were especially near the magic numbers mentioned above. As for water, one-molecule adsorbed ions were observed for $n = 13, 16, 21, 22, 25,$ and 27 . It was already reported that a water molecule was efficiently adsorbed on $\text{Na}_n\text{F}_{n-1}^+$ with one n smaller than the magic numbers, such as $n = 13$ and 22 [6,9,28]. This tendency was easily explained by the water adsorption on the defect sites of the cuboid structures which are formed at the magic number clusters. In addition, cluster ions with more than two n smaller ($n = 21$) or larger ($16, 25,$ and 27) than the magic sizes were also found to form one-water adsorbed ions, whereas no water was adsorbed on the ions with one n larger than the magic numbers, $n = 15$ and 24 . It should also be noted that three water molecules were adsorbed only on $\text{Na}_{19}\text{F}_{18}^+$. This observation was partly consistent with the former theoretical calculations [18]: An optimized structure of the $\text{Na}_{19}\text{F}_{18}^+$ ion has at least two cage site which can accept a small molecule like water for each. In the reaction with methanol, a methanol was adsorbed on the $\text{Na}_n\text{F}_{n-1}^+$ cluster ions with $n = 13, 16, 21,$ and 22 . Thus in addition to the sizes ($n = 13$ and 22) with one n smaller than the magic numbers, the ions with two ($n = 21$) and three ($n = 22$) n smaller were also found to form molecular adsorbed ions. Although this feature was almost consistent with water adsorption, there was a marked difference in the sizes of molecular-adsorbed cluster ions between water and methanol: No methanol-adsorbed ions were found for the larger neighboring sizes than the magic number at $n = 23$. This result may be due to the fact that methanol adsorbed ions may be unstable than water adsorbed ions at these sizes probably because the binding energy of methanol is smaller than that of water.

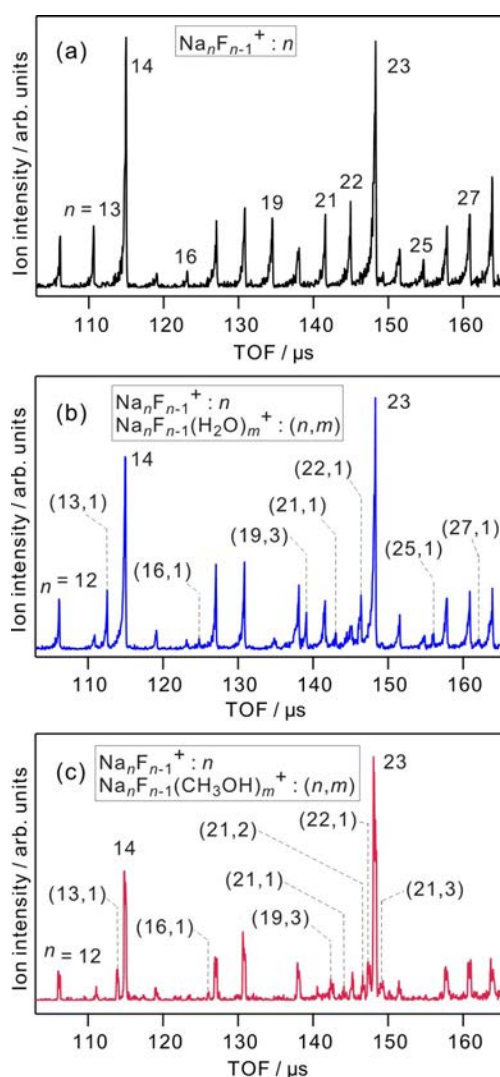


Fig. 4. TOF mass spectra of $\text{Na}_n\text{F}_{n-1}^+$ cluster ions for $n = 12$ -28 at different ion-drift cell conditions. (a) Without reactions (only He buffer gas), (b) reacted with water (0.2 % in He), and (c) reacted with methanol (1 % in He).

Conclusion

Structures and adsorption reactions were studied for sodium halide cluster ions. As for geometrical structures, $\text{Na}_n\text{F}_{n-1}^+$, $\text{Na}_n\text{I}_{n-1}^+$, $\text{Na}_{n-1}\text{F}_n^-$, and $\text{Na}_{n-1}\text{I}_n^-$, was examined for n up to 14 by a combination of ion mobility mass spectrometry (IM-MS) and quantum chemical calculations. The comparison between the experimental cross sections measured in IM-MS and theoretical ones, most of the ions have substructures of bulk face-centered-cubic crystals. Cuboid ions with near regular hexahedron such as $n = 14$ ($3 \times 3 \times 3$), 23 ($3 \times 3 \times 5$), and 38 ($3 \times 5 \times 5$) were also assigned as magic numbers in the mass spectra. In addition, non-rock-salt "cage" type structures in which one excess atom is encapsulated into the sodium halide cuboid lattice were also found to be stable for $n = 7$ and 10 in $\text{Na}_n\text{F}_{n-1}^+$, $\text{Na}_n\text{I}_{n-1}^+$, and $\text{Na}_{n-1}\text{F}_n^-$. Also the stable geometric structures of above four cluster systems were examined systematically in order to obtain the dependence of composite ion sizes on the stable structures. As for the $\text{Na}_{n-1}\text{F}_n^-$ anions and the $\text{Na}_n\text{I}_{n-1}^+$ cations, the cage type structures similar to those of Na_7F_6^+ and $\text{Na}_{10}\text{F}_9^+$ were observed at $n = 7$ and 10 . However, fairly distorted cage structures were assigned for any size of Na_6I_7^- and $\text{Na}_9\text{I}_{10}^-$ anions than other systems. The normal cage structures are unstable for the nanocrystal ions with large caged ions (excess atomic ions) of I^- (ionic radius of 2.06 Å), whereas they are stable for small caged ions such as Na^+ (1.16 Å) and F^- (1.19 Å). The experiment of water and methanol adsorption reactions on $\text{Na}_n\text{F}_{n-1}^+$ ions also showed that the water molecule is highly reactive at specific cluster size, e.g., $n = 13$ and 22 .

Acknowledgments

Part of the experiments were done by Riki Hotta and Shun Miyazaki in The Department of Chemistry, Tohoku University. This work was mainly supported by The Salt Research Science Foundation, Grant Nos. 1418, 1524, and 1621, and in part by a Grant-in-Aid for Scientific Research from the Japan Society for the Promotion of Science (JSPS). Theoretical calculations were performed using the Research Center for Computational Science, Okazaki, Japan.

References

- [1] T. P. Martin, *Phys. Rep.* **95**, 167 (1983).
- [2] R. L. Whetten, *Acc. Chem. Res.* **26**, 49 (1993).
- [3] E. C. Honea, M. L. Homer, P. Labastie, and R. L. Whetten, *Phys. Rev. Lett.* **63**, 394 (1989).
- [4] R. D. Beck, P. St. John, M. L. Homer, and R. L. Whetten, *Science* **253**, 879 (1991).
- [5] X. Li, R. D. Beck, and R. L. Whetten, *Phys. Rev. Lett.* **68**, 3420 (1992).
- [6] M. L. Homer, F. E. Livingston, and R. L. Whetten, *J. Am. Chem. Soc.* **114**, 6558 (1992).
- [7] J. L. Chen, C. S. Wang, K. A. Jackson, and M. R. Pederson, *Phys. Rev. B* **45**, 1927 (1992).
- [8] R. Ahlrichs and C. Ochsenfeld, *Ber. Bunsenges. Phys. Chem.* **96**, 1287 (1992).
- [9] M. L. Homer, F. E. Livingston, and R. L. Whetten, *J. Phys. Chem.* **99**, 7604 (1995).
- [10] R. N. Barnett and U. Landman, *J. Phys. Chem.* **100**, 13950 (1996).
- [11] P. Dugourd, R. R. Hudgins, and M. F. Jarrold, *Chem. Phys. Lett.* **267**, 186 (1997).
- [12] R. R. Hudgins, P. Dugourd, J. M. Tenenbaum, and M. F. Jarrold, *Phys. Rev. Lett.* **78**, 4213 (1997).
- [13] M. Maier-Borst, P. Löffler, J. Petry, and D. Kreisler, *Z. Phys. D* **40**, 476 (1997).
- [14] G. Grégoire, M. Mons, C. D. Lardeux, and C. Jouvet, *Eur. Phys. J. D* **1**, 5 (1998).
- [15] A. Aguado, A. Ayuela, J. M. López, and J. A. Alonso, *Phys. Rev. B* **58**, 9972 (1998).
- [16] M. Lintuluoto, *J. Phys. Chem. A* **104**, 6817 (2000).
- [17] S. Yamabe, H. Kouno, and K. Matsumura, *J. Phys. Chem. B* **104**, 10242 (2000).
- [18] M. Lintuluoto, *J. Mol. Struct. (THEOCHEM)* **540**, 177 (2001).
- [19] M. P. Ince, B. A. Perera, and M. J. Van Stipdonk, *Int. J. Mass Spectrom.* **207**, 41 (2001).
- [20] D. J. Fatemi, and L. A. Bloomfield, *Phys. Rev. A* **66**, 013202 (2002).
- [21] N. Haketa, K. Yokoyama, H. Tanaka, and H. Kudo, *J. Mol. Struct. (THEOCHEM)* **577**, 55 (2002).

- [22] Q. Zhang, C. J. Carpenter, P. R. Kemper, and M. T. Bowers, *J. Am. Chem. Soc.* **125**, 3341 (2003).
- [23] F. K. Fatemi, A. J. Dally, and L. A. Bloomfield, *Phys. Rev. Lett.* **91**, 073401 (2003).
- [24] S. Zhang and N. Chen, *Physica B* **325**, 172 (2003).
- [25] F. Misaizu, M. Tsuruta, H. Tsunoyama, A. Furuya, K. Ohno, and M. Lintuluoto, *J. Chem. Phys.* **123**, 161101 (2005).
- [26] C. Bréchignac, Ph. Cahuzac, F. Calvo, G. Durand, P. Feiden, J. Leygnier, *Chem. Phys. Lett.* **405**, 26 (2005).
- [27] F. A. Fernandez-Lima, C. Becker, K. Gillig, W. K. Russell, M. A. C. Nascimento, and D. H. Russell, *J. Phys. Chem. A* **112**, 11061 (2008).
- [28] M. Tsuruta, A. Furuya, K. Ohno, M. Lintuluoto, and F. Misaizu, *J. Phys. Chem. A* **114**, 1432 (2010).
- [29] E. A. Mason and E. W. McDaniel, *Transport Properties of Ions in Gases*, Wiley (1988).
- [30] H. E. Revercomb and E. A. Mason, *Anal. Chem.* **47**, 970 (1975).
- [31] G. A. Eiceman and Z. Karpas, *Ion Mobility Spectrometry* (CRC press, 2005).
- [32] C. L. Wilkins and S. Trimpin, *Ion Mobility Spectrometry-Mass Spectrometry: Theory and Applications* (CRC press, 2010).
- [33] K. Ohshimo, T. Komukai, R. Moriyama, and F. Misaizu, *J. Phys. Chem. A* **118** (22), 3899 (2014).
- [34] K. Ohshimo, T. Takahashi, R. Moriyama, and F. Misaizu, *J. Phys. Chem. A* **118**, 9970 (2014).
- [35] K. Ohshimo, T. Komukai, T. Takahashi, N. Norimasa, J. W. J. Wu, R. Moriyama, K. Koyasu, and F. Misaizu, *Mass Spectrom.* **3**, S0043 (2014). (7 pages)
- [36] M. J. Frisch *et al.*, GAUSSIAN 09, Revision D.01, Gaussian: Wallingford, CT, USA, 2013.
- [37] M. F. Mesleh, J. M. Hunter, A. A. Shvartsburg, G. C. Schatz, and M. F. Jarrold, *J. Phys. Chem.* **100**, 16082 (1996).
- [38] R. D. Shannon, *Acta Cryst. A* **32**, 751 (1976).